Pattern of seismicity in the Lucanian Apennines and foredeep (Southern Italy) from recording by SAPTEX temporary array

Alberto Frepoli, Francesca Romana Cinti, Laura Amicucci, Giovanni Battista Cimini, Pasquale De Gori and Simona Pierdominici
Istituto Nazionale di Geofisica e Vulcanologia, Roma, Italy

Abstract
The deployment of a temporary seismic network in Southern Italy during 2001-2004 (the SAPTEX array, Southern APennine Tomography EXperiment) allowed us to relocate the hypocenters of Southern Apennines earthquakes with low uncertainty among the location parameters. The best array distribution of the SAPTEX network for the analysis of seismicity in the Lucanian Apennines and foredeep was reached in the first two years of recording. The SAPTEX data were merged with those of the Italian National Seismic Network (RSNC) operated by the Istituto Nazionale di Geofisica e Vulcanologia (INGV). For the hypocenters computation of events in the upper Agri Valley we also included *P*- and *S*- waves arrivals from the local Eni-Agip network. The seismicity for the Lucanian Apennines and foredeep in the analyzed period has magnitudes ranging from 2.0 to 4.1. A major finding is the identification of two different crustal domains: the westernmost characterizing the chain, mostly with shallow earthquakes (within about 20 km of depth), and the easternmost one belonging to the outer margin of the chain and to the foredeep, with deeper seismicity (mostly between 20-40 km of depth). Thirty fault-plane solutions were computed and used for stress inversion; most of them are related to earthquakes within the chain sector and indicate a generalized NE-SW extension. Moreover, the dense network allowed us to improve the location of events relative to two low magnitude sequences which occurred in the study period.

Key words *seismicity – seismic network – seismotectonics – Lucanian Apennines – Lucanian foredeep – Southern Italy*

1. Introduction

The SAPTEX passive array was planned by Cimini *et al*. (2005) and represented the longest deployment of portable seismic stations carried out in Southern Italy. The main goal of the experiment was to better resolve the crustal and upper mantle structure beneath Southern Italy. In fact, the paucity of permanent stations in this region was still remarkable thus preventing high-resolution tomographic studies, detail definition of the lithosphere-astenosphere structure and precise hypocentral determination. The three years long experiment provided the extraction of numerous digital waveforms of local, regional and teleseismic events (for additional details on the network see Cimini *et al*., 2005).

In this work we benefit from using data recorded by SAPTEX temporary stations to an-

Mailing address: Dr. Alberto Frepoli, Istituto Nazionale di Geofisica e Vulcanologia, Via di Vigna Murata 605, 00143 Roma, Italy; e-mail: frepoli@ingv.it

alyze the seismicity occurring in the Lucanian area, definitively a seismically active area of Southern Italy (fig. 1). Based on the instrumental catalogues (1981-2002 from Castello *et al*., 2005), a 30-40 km wide belt of seismicity characterizes the Lucanian Apennines and its outer margin, where earthquakes reach the highest magnitudes. Conversely, along the external zones of the Bradano foredeep and Apulia foreland, low to moderate-size earthquakes are infrequent and sparse (fig. 1). Most of the earthquakes are limited to the upper crust (hypocentral depths <20 km), defining the depth extent of the seismogenic layer of this region. A dense cluster of earthquakes surrounds the city of Potenza (referred to as the Potentino area), a second is located in the Irpinia region, and a third cluster is in the northwestern part of the Pollino (referred to as the Castelluccio area). An area of very scarse seismicity extends for about 25 km in the NW-SE direction within the Apenninic Chain from the Vallo di Diano and upper Agri Valley. In the last 25 years, the most destructive event was the 1980 Irpinia event (M_w=6.9; see table 1) with normal mechanism of rupture (Boschi *et al*., 1990). A significant earthquake occurred in 1990 (M_w=5.7) in the Potentino area (Azzara *et al*., 1993; Ekström, 1994); aftershock depths of this sequence range between 15 and 25 km on an E-W oriented strike-slip structure. A similarly located event occurred in 1991 (M_w=5.2; Ekström, 1994). The different focal solutions obtained for the Irpinia inland event and the two external Potentino events, suggest the presence of a transition zone between pure extensional, to the west, and strike-slip regime, to the east. The strike-slip, M_w 5.7, 2002 Molise earthquake located to the east of the chain at 20 km depth (Di Bucci and Mazzoli, 2003; Valensise *et al*., 2004; Di Luccio *et al*., 2005) would support this setting also northwest of the study area. Finally, the 1998, M_w=5.6 Castelluccio event with pure normal focal mechanism, hit the northwestern side of

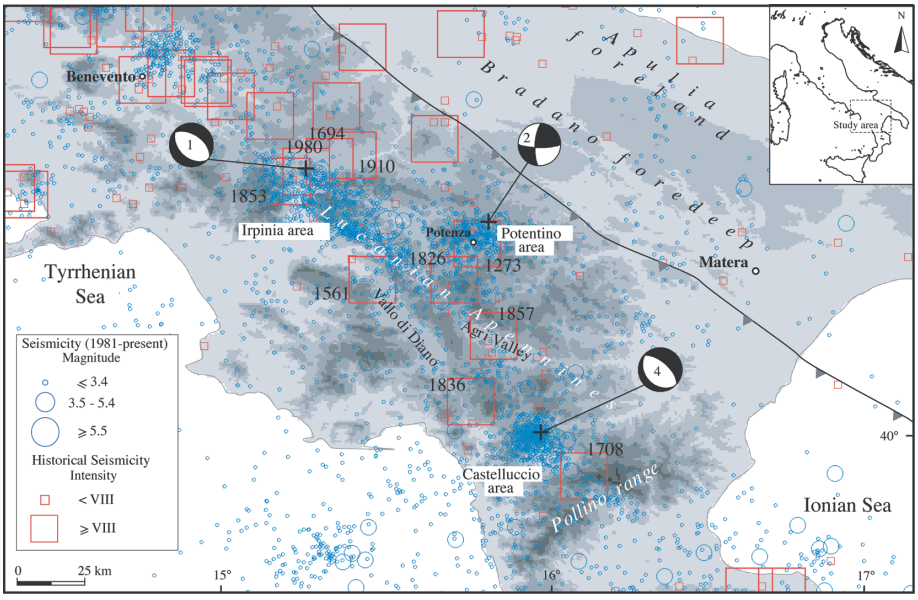

Fig 1. Seismicity map of Southern Italy (Castello *et al*., 2005; CPTI Working Group, 1999) from 1981 to present. The dates of occurrence for the largest events are indicated. The available CMT (Centroid Moment Tensor) solutions of the earthquakes of $M \geq 5.0$ are also shown (Pondrelli *et al*., 2002). Numbered focal spheres correspond to events in table I.

Table I. Parameters of the largest instrumental earthquakes in the Southern Apennines (parameters of the Irpinia event are from Amato and Selvaggi (1993), of the two Potenza earthquakes are from Ekström (1994), of the Castelluccio-Lauria are from Harvard CMT Catalogue). The CMT (Centroid Moment Tensor) solutions of these earthquakes are shown in fig. 1, except for the unavailable mechanism of event no. 3.

No.	Epicenter	Date	Latitude °N	Longitude °E	M_W	Depth (km)
1	Irpinia	23/11/1980	40.724	15.373	6.9	10
2	Potenza	05/05/1990	40.775	15.766	5.7	9-13
3	Potenza	26/05/1991	40.730	15.765	5.2	11
4	Castelluccio-Lauria	09/09/1998	40.015	15.947	5.6	10

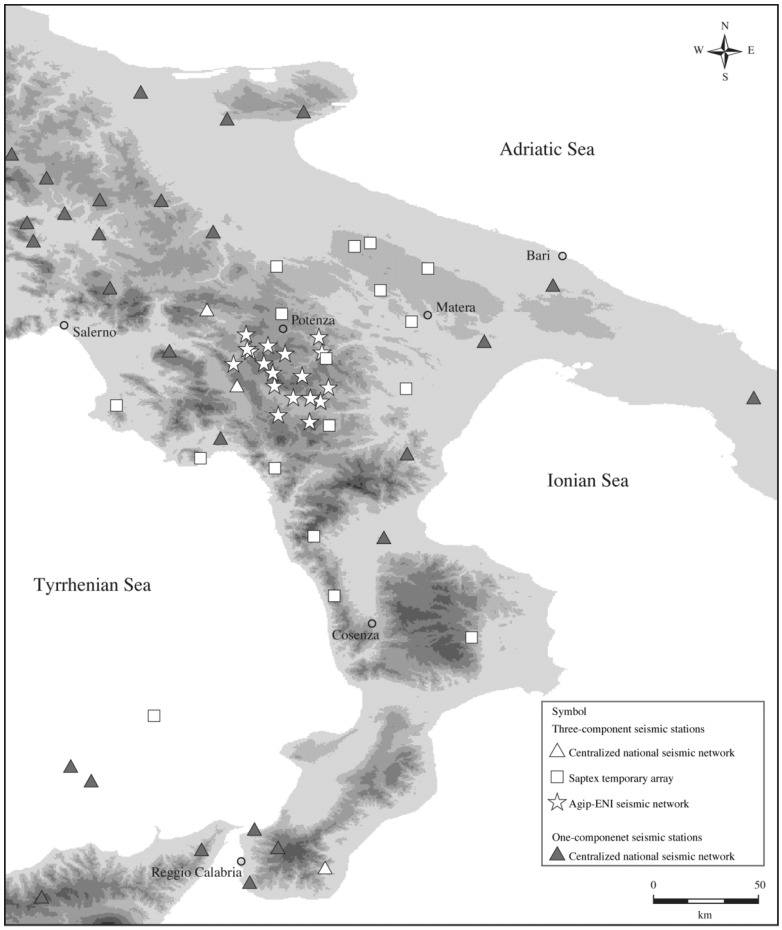

Fig. 2. Map of seismic stations used in this study. White triangles are the three-components permanent stations of the Italian National Seismic Network (RSNC), white square are the three-components temporary stations of the SAPTEX array, white stars are the short-period three-components stations of the Eni-Agip local network in the Agri Valley area and dark-grey triangles are the one-component stations of the RSNC.

the Pollino range (Michetti *et al*., 2000; Pondrelli *et al*., 2002). Similarly to the recent seismicity, most of the destructive events reported in the historical catalogue (CPTI Working Group, 1999) are located within the Apenninic Chain (fig. 1); among them, the largest is the 1857 (M_a=7.0) occurring south of Potenza, in the Agri Valley.

The availability of a denser station coverage provided by the SAPTEX array with respect to that of the national network RSNC, represented a good opportunity for highlighting details of «earthquake structures» in the Lucanian area and to investigate the region's active tectonics. We could determine high quality hypocentral parameters and fault-plane solutions of local earthquakes recorded at the temporary SAPTEX network in the period 2001-2002, merged with the RSNC data and the Eni-Agip local network (fig. 2). We performed the picking of SAPTEX phases and re-picked those from RSNC seismic network. The Eni-Agip local network provided us directly the *P*- and *S*- time arrivals. The work is developed in the following steps: location of events which occurred in the period June 2001-December 2002, 3D analysis of the seismicity pattern, analysis of sequences, focal mechanisms computation and inversion of fault-plane solutions for stress field determination. In conclusion, we discuss the results integrating the seismic data collected with a seismic profile.

2. Earthquake data

We analyzed the seismicity of the Lucanian Region in the time period between June 2001 and December 2002. The earthquakes were recorded at the SAPTEX temporary array and the RSNC network. For the analysis of the seismicity in the upper Agri Valley and surrounding areas, the *P*- and *S*-wave arrival time readings from Eni-Agip seismic network (fig. 2) were also used. The recording mode of the SAPTEX stations was continuous, while the RSNC and Eni-Agip networks record as trigger mode. The list of the local events was extracted from the INGV Seismic Bulletin (at www.ingv.it/~roma/frames/frame-boll.html). During 2002 the SAPTEX array reached its maximum configuration with up to 12 operating stations (additional details in Cimini *et al*., 2005). The seismic stations are the three-component Lennarz 5 s sensors of the SAPTEX seismic experiment, the one-component S-13 sensors of the RSNC (with the exception of two stations; see fig. 2), and the three-component Lennarz Lite 1 s sensors of the Eni-Agip seismic network.

2.1. *Hypocentral locations*

Locations were computed with the HYPOELLIPSE code (Lahr, 1989) using the one-dimensional velocity model of Chiarabba *et al*. (2005). We calculated an average V_p/V_s ratio equal to 1.82 using a modified Wadati method (fig. 3a). A well-constrained V_p/V_s ratio strongly helped in providing reliable hypocentral depth estimates.

A total of 204 events occurred between June 2001 and the end of 2002 within the study area and they have been relocated. The events have a magnitude Md ranging from 2.0 to 4.1 (INGV Seismic Bulletin) and their epicentral locations occur within a 260 km×180 km area (within 15.0°E-17.4°E and 39.8°N-41.2°N).

From the collected seismograms, the arrival times of 2677 *P*- and 1226 *S*-phases were picked, giving a total of 3903 travel times. To provide some quantitative assessment of the reading uncertainty (σ_{pick}) and hence determination of reasonable data weights ($1/\sigma^2_{\text{pick}}$), we assigned a quality index to each arrival (table II). *S*-phases were picked only on the three-component stations. Figure 3b shows the errors location, gap, residual values and phase numbers relative to the whole data set of events.

We decided to reject the earthquakes with horizontal (ERH) and vertical (ERZ) location errors larger than 1.5 and 2.2 km, respectively, and with azimuthal gaps larger than 195°. The locations of the 120 remaining events are shown in fig. 4 and earthquake parameters are listed in table III. The average error on the horizontal direction is 0.25 km and on the vertical is 0.46 km (table III).

Based on the estimated hypocentral depths, most of the Lucanian Region seismicity occurs within the upper crust, in the first 20 km. Only

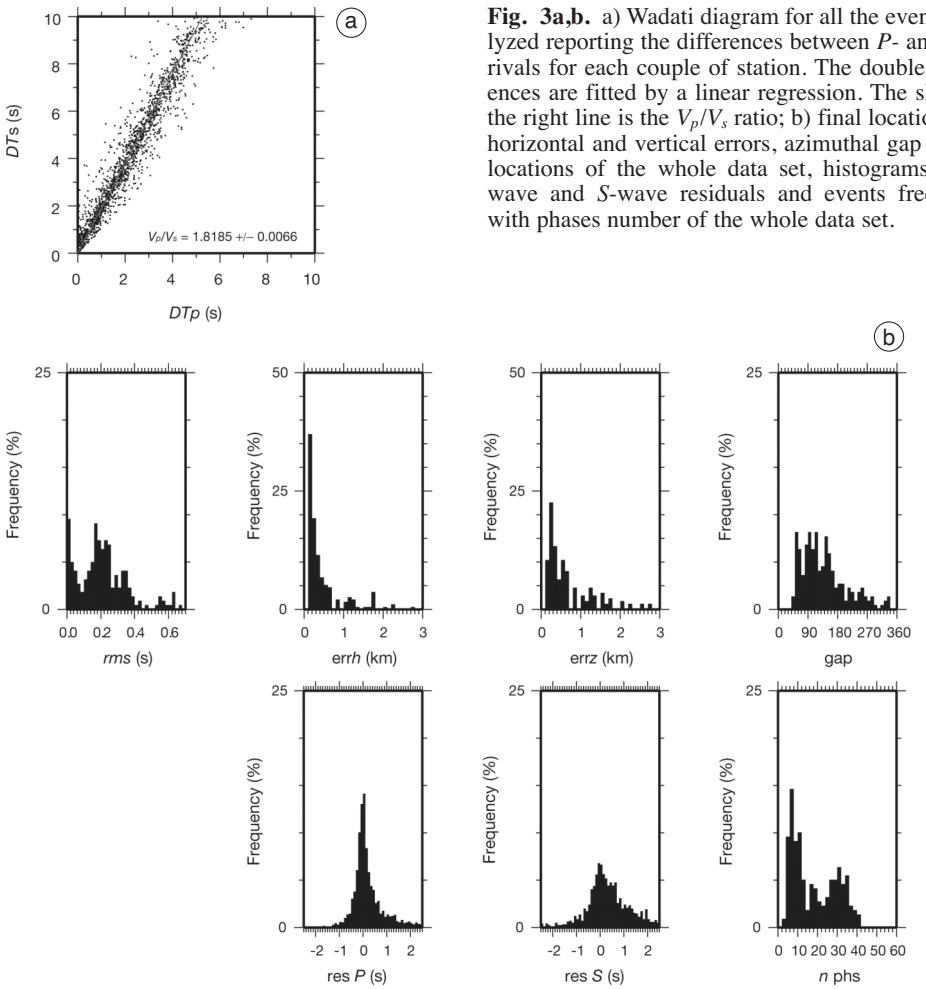

Fig. 3a,b. a) Wadati diagram for all the events analyzed reporting the differences between *P*- and *S*-arrivals for each couple of station. The double differences are fitted by a linear regression. The slope of the right line is the V_p/V_s ratio; b) final location rms, horizontal and vertical errors, azimuthal gap for the locations of the whole data set, histograms of *P*-wave and *S*-wave residuals and events frequency with phases number of the whole data set.

Table II. Picking accuracy quality index assigned to each *P*- and *S*-arrival.

a quality	b quality	c quality	d quality
0.04 s (1879 picks)	0.10 s (753 picks)	0.20 s (621 picks)	0.40 s (650 picks)

17 out of the 120 detected events have hypocenters in the lower crust, ranging between 21 and 33 km. Six subcrustal earthquakes were detected at depths between 37 and 92 km.

The analysis of the crustal seismicity indicates two regions with different pattern of earthquake epicentral distribution and depths (see fig. 4, vertical cross sections AB and CD). One region is centered along the axis of the Apenninic Chain for a width of about 40 km, and the other includes the eastern outer margin of the chain and the foredeep.

The seismicity within the region of the Apenninic Chain defines two main clusters. The northern one is limited to the Irpinia area and Pergola-Melandro Basin, the second to the south in the upper Agri Valley and the Castelluccio

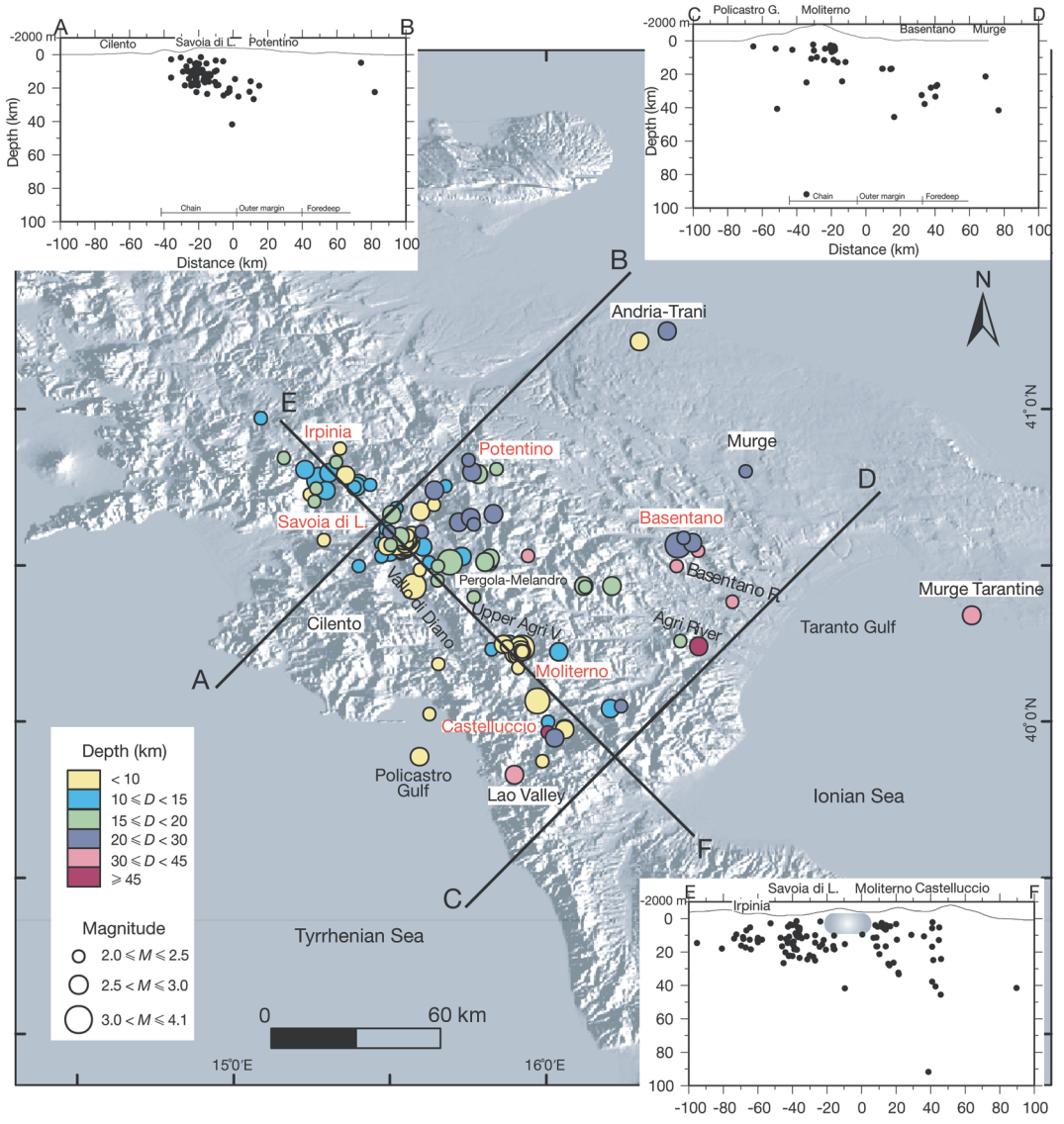

Fig. 4. Epicentral locations, depths and magnitudes of the local seismicity (120 earthquakes) selected for this study in the Lucanian Region. The three cross-sections in the insets show the projection of the hypocenters (see locations in the map). The maximum earthquake distance from sections AB, CD and EF is 30 km, 50 km and 200 km, respectively. Topography is vertically exaggerated.

area. Within the latter, hypocenters are generally shallower with respect to the north, mostly occurring within the first 15 km of crust. Between these two areas, there is a strip 25 km long along the axis of the chain where no shallow earthquakes (depth <10 km, see shaded area in section EF in fig. 4) occurred during the investigated period; beneath this strip where the seismicity is

Table III. Hypocentral parameters, duration magnitude, azimuthal gap, location errors (rms, ERH, ERZ), total number of *P*- and *S*-phases used for location, location quality and geographic area of the 120 earthquakes selected in this study.

No.	Date (d/m/yr)	O.T. (h/min)	Lat °N	Long °E	Depth (km)	M_d	Gap	rms (s)	ERH (km)	ERZ (km)	Number of *P* and *S* phases	*Q*	Region
1	08/07/01	09:49	40.7567	15.4363	12.7	2.4	162	0.11	0.4	0.3	7	A	Irpinia
2	25/07/01	09:22	39.9993	16.0058	10.7	2.3	125	0.03	0.9	1.4	7	B	Castelsaraceno
3	28/07/01	05:05	40.8722	15.3398	9.5	2.2	166	0.03	0.2	0.3	9	A	Irpinia
4	12/08/01	09:12	40.805	15.2282	12.1	2.6	124	0.04	0.3	0.7	9	A	Irpinia
5	14/08/01	00:55	40.7958	15.3055	11.2	3.0	86	0.41	0.1	0.2	35	A	Irpinia
6	17/08/01	01:45	40.6832	15.5205	11.6	2.5	109	0.05	0.4	0.4	10	A	Irpinia
7	20/08/01	06:01	40.4325	15.576	1.7	3.3	58	0.47	0.1	0.1	24	A	Vallo di Diano
8a	14/09/01	08:02	40.6382	15.7203	24.5	2.8	98	0.19	0.2	0.2	30	A	Potentino
9	17/09/01	21:04	40.9703	15.0873	14.7	2.3	156	0.01	0.5	0.9	4	A	Irpinia
10a	30/09/01	23:44	40.223	16.04	12.6	2.7	111	0.34	0.1	0.1	28	A	S. Martino d'Agri
11	07/10/01	08:38	40.509	15.626	14.4	2.3	187	0.01	0.4	0.5	6	A	Brienza
12	08/10/01	14:42	40.4967	15.3997	13.8	2.2	150	0.06	0.9	1.4	5	B	Alburni Mts
13a	13/10/01	18:57	40.45	15.652	18.6	2.2	187	0.18	0.2	0.3	10	A	Brienza
14	13/10/01	23:32	40.7493	15.3862	14.1	2.2	153	0.06	1.2	1.8	5	B	Irpinia
15	23/10/01	11:05	40.8427	15.1617	18.1	2.3	137	0.01	0.6	1.4	6	B	Irpinia
16	27/10/01	12:09	41.2147	16.298	4.9	2.7	146	0.11	0.6	0.4	19	A	Andria
17a	04/11/01	10:22	40.4313	16.1243	16.8	2.5	75	0.38	0.1	0.2	29	A	Stigliano
18a	04/11/01	10:28	40.434	16.1197	16.6	3.0	53	0.42	0.1	0.2	41	A	Stigliano
19	04/11/01	23:49	40.4858	15.596	9.9	2.4	58	0.34	0.1	0.1	31	A	Brienza
20a	13/11/01	13:21	40.53	15.942	41.8	2.4	45	0.60	0.1	0.2	38	A	Central Lucania
21	21/11/01	06:10	40.5127	15.8157	18.4	2.8	77	0.24	0.1	0.2	27	A	Calvello
22a	21/11/01	06:21	40.5217	15.8213	18.1	2.7	94	0.22	0.1	0.2	26	A	Calvello
23a	09/12/01	12:15	40.7722	15.275	12.1	3.2	96	0.30	0.1	0.2	29	A	Irpinia
24	13/12/01	04:33	40.746	15.264	17.4	2.3	144	0.01	0.4	1.0	5	A	Irpinia
25	19/12/01	06:36	39.8865	15.5945	3.4	2.7	166	0.38	0.3	0.4	14	A	Policastro Gulf
26a	02/01/02	02:09	40.753	15.392	11.6	2.7	82	0.28	0.1	0.2	19	A	Irpinia
27a	02/01/02	02:17	40.7608	15.3995	12.8	2.8	80	0.27	0.1	0.2	32	A	Irpinia
28	14/01/02	01:47	40.183	15.6547	9.7	2.5	151	0.15	0.2	0.5	11	A	Morigerati
29a	15/01/02	00:06	40.7982	15.7622	22.2	2.6	155	0.32	0.1	0.4	24	A	Potentino
30	15/01/02	00:11	40.7913	15.7828	16.0	2.6	151	0.20	0.2	0.8	14	A	Potentino
31	15/01/02	01:29	40.836	15.7505	26.7	2.4	122	0.48	0.3	0.9	18	A	Potentino
32	22/01/02	12:43	40.5578	15.606	10.7	2.6	114	0.15	0.2	0.2	20	A	Savoia di Lucania
33	30/01/02	19:42	40.8	16.6382	21.3	2.0	124	0.16	0.1	0.5	16	A	Murge
34a	08/02/02	04:38	40.2418	15.913	3.7	2.6	47	0.32	0.1	0.3	22	A	Moliterno
35	11/02/02	21:09	40.8288	15.3283	16.2	2.5	153	0.25	0.3	0.4	23	A	Irpinia
36	13/02/02	04:20	39.8305	15.8973	40.6	2.6	126	0.34	0.4	0.3	18	A	Lao Valley
37	14/02/02	02:34	40.7403	15.6427	20.1	2.6	160	0.08	0.3	0.9	12	A	Potentino

Table III (*continued*)**.**

No.	Date (d/m/yr)	O.T. (h/min)	Lat °N	Long °E	Depth (km)	M_d	Gap	rms (s)	ERH (km)	ERZ (km)	Number of *P* and *S* phases	*Q*	Region
38a	26/02/02	17:12	40.2278	15.9193	4.6	2.6	95	0.19	0.1	0.1	29	A	Moliterno
39	03/03/02	18:30	40.539	15.536	11.7	2.1	163	0.12	0.5	2.1	6	B	Savoia di Lucania
40	04/03/02	00:44	40.7528	15.6788	14.6	2.4	129	0.16	0.3	0.9	12	A	Potentino
41	16/03/02	02:01	40.5803	15.288	3.0	2.2	112	0.26	0.2	0.1	8	A	Alburni Mts
42a	17/03/02	04:53	40.2335	15.9135	3.0	2.8	53	0.37	0.1	0.3	18	A	Moliterno
43	17/03/02	06:09	40.231	15.8257	11.5	2.5	83	0.26	0.3	1.8	8	B	Moliterno
44	20/03/02	17:34	40.7257	15.2443	7.1	2.4	116	0.16	0.3	1.8	11	B	Irpinia
45	24/03/02	00:11	40.2408	16.4877	45.5	2.8	153	0.47	0.2	0.2	27	A	Lower Agri Valley
46	28/03/02	09:59	40.34	17.361	41.6	2.8	139	0.19	0.4	1.9	13	B	Murge Tarantine
47	02/04/02	04:22	40.246	15.863	4.1	2.7	56	0.56	0.1	0.2	27	A	Moliterno
48	04/04/02	22:07	40.5068	15.806	10.2	2.3	113	0.31	0.3	0.8	23	A	Brienza
49a	13/04/02	08:44	40.5112	15.8043	16.4	2.7	68	0.22	0.1	0.2	35	A	Calvello
50a	13/04/02	10:48	40.1728	15.9105	4.7	2.5	66	0.24	0.1	0.2	31	A	Moliterno
51a	13/04/02	17:04	40.5635	16.4205	28.0	3.3	70	0.36	0.1	0.1	47	A	Basentano
52a	13/04/02	17:16	40.4965	16.4173	32.4	2.4	100	0.25	0.2	0.1	37	A	Basentano
53	13/04/02	19:52	40.5875	16.4397	27.2	2.2	117	0.20	0.5	0.9	18	A	Basentano
54	13/04/02	20:28	40.5452	16.4855	33.3	2.5	106	0.25	0.3	0.1	21	A	Basentano
55	13/04/02	20:31	40.5717	16.469	26.4	2.6	99	0.11	0.2	0.5	20	A	Basentano
56	18/04/02	20:56	40.5738	15.5463	11.1	4.1b	54	0.30	0.1	0.1	46	A	Savoia di Lucania
57	18/04/02	20:58	40.595	15.5697	9.2	2.8	115	0.37	0.1	0.2	23	A	Savoia di Lucania
58	18/04/02	21:00	40.5723	15.5452	8.5	3.2	55	0.37	0.1	0.2	37	A	Savoia di Lucania
59	18/04/02	21:36	40.567	15.5512	7.0	3.1	68	0.32	0.1	0.3	34	A	Savoia di Lucania
60	18/04/02	21:37	40.5778	15.558	5.6	2.7	110	0.40	0.1	0.2	27	A	Savoia di Lucania
61a	18/04/02	22:58	40.5698	15.5485	5.6	3.0	55	0.37	0.1	0.2	36	A	Savoia di Lucania
62	18/04/02	23:19	40.5725	15.5545	9.8	3.1	54	0.32	0.1	0.2	37	A	Savoia di Lucania
63	18/04/02	23:56	40.6173	15.4867	12.3	2.2	113	0.23	0.4	0.4	11	A	Savoia di Lucania
64	19/04/02	22:12	40.5783	15.545	8.8	2.6	93	0.31	0.2	1.1	13	B	Savoia di Lucania
65	20/04/02	20:37	40.5943	15.5578	1.5	2.3	114	0.21	0.1	0.3	12	A	Savoia di Lucania
66	20/04/02	23:31	40.5815	15.556	5.5	2.6	96	0.24	0.2	0.2	26	A	Savoia di Lucania
67	21/04/02	00:57	40.5737	15.5197	9.0	3.1	75	0.48	0.1	0.2	36	A	Savoia di Lucania
68	21/04/02	01:01	40.5918	15.5333	18.5	2.6	111	0.06	0.3	0.9	9	A	Savoia di Lucania
69	21/04/02	23:39	40.573	15.5418	5.1	3.5	60	0.33	0.1	0.1	50	A	Savoia di Lucania
70	23/04/02	15:58	40.2545	15.883	11.2	2.4	54	0.29	0.1	0.2	30	A	Moliterno
71	23/04/02	21:14	40.6073	15.4977	22.3	2.4	104	0.04	0.3	1.2	9	A	Savoia di Lucania
72	25/04/02	15:06	40.2578	16.4288	16.9	2.4	155	0.28	0.3	0.2	33	A	Lower Agri Valley
73	26/04/02	19:14	40.2388	15.8745	4.9	2.3	66	0.17	0.1	0.1	28	A	Moliterno
74	29/04/02	03:19	40.561	15.5443	5.6	3.2	56	0.31	0.1	1.2	32	B	Savoia di Lucania
75	29/04/02	19:23	40.4337	16.2103	16.7	2.8	89	0.25	0.1	0.3	32	A	Stigliano
76a	04/05/02	09:41	40.6617	15.507	16.6	2.7	62	0.24	0.1	0.2	35	A	Irpinia

Table III (*continued*)**.**

No.	Date (d/m/yr)	O.T. (h/min)	Lat °N	Long °E	Depth (km)	M_d	Gap	rms (s)	ERH (km)	ERZ (km)	Number of *P* and *S* phases	*Q*	Region
77	05/05/02	06:40	40.6067	15.6013	23.5	2.4	57	0.15	0.1	0.2	30	A	Savoia di Lucania
78	08/05/02	19:29	40.0662	15.9725	9.8	3.1	62	0.37	0.1	0.3	37	A	Castelluccio
79	08/05/02	20:46	40.0413	16.2057	13.0	2.6	78	0.35	0.2	0.2	35	A	Francavilla in Sinni
80	08/05/02	22:36	40.0488	16.2392	24.2	2.5	80	0.45	0.1	0.3	33	A	Francavilla in Sinni
81	09/05/02	23:55	40.3832	16.5958	37.7	2.5	155	0.24	0.1	0.3	34	A	Lower Basentano
82a	12/05/02	20:20	40.652	15.7577	22.0	2.6	141	0.30	0.1	0.2	35	A	Potentino
83	18/05/02	19:04	40.5645	15.5023	17.7	2.4	107	0.14	0.2	0.6	10	A	Savoia di Lucania
84	26/05/02	08:46	40.5283	15.473	10.2	2.2	113	0.06	0.3	1.1	8	A	Savoia di Lucania
85	26/05/02	10:19	40.5423	15.4993	10.0	2.6	103	0.27	0.1	0.3	25	A	Savoia di Lucania
86	31/05/02	16:31	40.2243	15.8955	2.6	2.8	57	0.24	0.1	0.2	34	A	Moliterno
87a	07/06/02	05:47	39.9655	16.0048	91.8	2.2	105	0.58	0.2	0.5	28	A	Castelluccio
88	08/06/02	23:04	40.571	15.4717	14.5	2.4	93	0.30	0.1	0.3	24	A	Savoia di Lucania
89	09/06/02	09:27	40.2152	15.9237	3.9	2.3	76	0.32	0.1	0.2	25	A	Moliterno
90a	11/06/02	20:02	40.5093	15.6928	15.5	3.1	57	0.41	0.1	0.1	45	A	Brienza
91a	18/06/02	23:31	40.5272	15.7308	13.0	2.7	51	0.36	0.1	0.1	36	A	Calvello
92	23/06/02	21:41	41.2488	16.3867	22.4	2.8	158	0.19	0.2	0.4	26	A	Trani
93	08/07/02	08:12	40.703	15.259	18.4	2.5	153	0.10	0.6	1.6	14	B	Irpinia
94	11/07/02	03:36	39.873	15.9877	5.3	2.3	132	0.59	0.1	0.4	14	A	Castelluccio
95	13/07/02	11:49	39.9773	16.0587	5.7	2.9	87	0.21	0.1	1.0	31	A	Castelluccio
96	17/07/02	21:48	40.6725	15.5975	3.6	2.6	158	0.35	0.3	0.7	9	A	Irpinia
97	18/07/02	08:23	39.9467	16.0268	25.0	2.8	102	0.57	0.1	0.3	24	A	Castelluccio
98a	18/07/02	08:28	39.974	16.0582	2.3	2.8	88	0.27	0.1	0.3	24	A	Castelluccio
99	21/07/02	22:50	40.7392	15.2955	12.7	2.6	139	0.20	0.6	0.7	13	A	Irpinia
100	09/08/02	06:16	40.5622	15.4907	3.8	2.7	137	0.44	0.2	0.4	19	A	Savoia di Lucania
101	10/08/02	23:04	40.7868	15.3587	5.4	2.7	119	0.20	0.2	0.4	10	A	Irpinia
102	24/08/02	06:43	40.6307	15.7685	22.9	2.1	142	0.20	0.2	0.2	29	A	Potentino
103	01/09/02	06:43	40.694	15.6412	4.0	2.3	103	0.61	0.2	0.7	19	A	Irpinia
104a	03/09/02	01:45	40.4972	15.6535	16.8	2.5	78	0.23	0.1	0.1	36	A	Brienza
105	20/09/02	07:35	40.6642	15.8308	25.2	2.7	63	0.20	0.1	0.2	38	A	Potentino
106	30/09/02	04:24	40.0242	15.6265	4.6	2.5	193	0.18	0.2	0.3	28	A	Policastro Gulf
107	03/10/02	22:56	40.2245	15.93	5.7	2.5	61	0.23	0.1	0.1	34	A	Moliterno
108a	04/10/02	22:58	40.2353	15.9233	5.4	3.2	52	0.34	0.1	0.1	46	A	Moliterno
109a	06/10/02	02:43	40.2252	15.9195	5.9	2.3	60	0.25	0.1	0.1	35	A	Moliterno
110	08/10/02	18:26	40.5955	15.4873	11.0	2.4	95	0.52	0.1	0.5	26	A	Savoia di Lucania
111a	17/10/02	15:19	40.3975	15.7673	15.2	2.1	64	0.19	0.1	0.2	26	A	Marsico Vetere
112	06/11/02	20:07	40.574	15.554	6.9	2.3	108	0.35	0.1	0.4	26	A	Savoia di Lucania
113a	09/11/02	01:53	40.8077	15.8412	18.6	2.5	87	0.23	0.1	0.3	21	A	Potentino
114a	19/11/02	16:53	40.2268	15.9173	4.8	2.2	79	0.22	0.1	0.2	32	A	Moliterno
115	25/11/02	22:51	40.5935	15.5648	10.2	2.5	116	0.24	0.2	0.6	23	A	Savoia di Lucania

Table III (*continued*)**.**

No.	Date (d/m/yr)	O.T. (h/min)	Lat °N	Long °E	Depth (km)	M_d	Gap	rms (s)	ERH (km)	ERZ (km)	Number of *P* and *S* phases	*Q*	Region
116a	29/11/02	10:54	40.2158	15.9057	4.9	2.3	82	0.25	0.1	0.2	30	A	Moliterno
117a	30/11/02	01:19	40.2175	15.8975	4.2	2.8	82	0.25	0.1	0.2	30	A	Moliterno
118a	30/11/02	17:33	40.2162	15.9083	5.1	2.7	56	0.19	0.1	0.1	32	A	Moliterno
119	01/12/02	00:30	40.214	15.9197	6.7	2.5	62	0.17	0.1	0.3	30	A	Moliterno
120	28/12/02	00:22	40.2235	15.9233	4.4	2.2	61	0.14	0.1	0.2	31	A	Moliterno

a – events with fault-plane solutions (see table IV); b – local magnitude (M_l).

completely absent, a few events at the eastern border of the chain are spread at depths larger than 10 km (see cross-section EF in fig. 4). West of the chain, the crustal seismicity is almost absent (the Cilento area and the Policastro Gulf).

During the first two years of the SAPTEX deployment, a seismic sequence, named Savoia di Lucania in table III and fig. 5a, was recorded at the north edge of the Pergola-Melandro Basin (fig. 4). This sequence started with the April 18, 2002, M_l=4.1, mainshock located at 11 km depth, followed by 24 aftershocks with magnitudes larger than 2.2 (table III). The aftershock epicenters show a cluster slightly elongated in a SW-NE direction (fig. 5a). Most of the hypocenters occur between 4 and 11 km and cluster at shallower depths with respect to the mainshock. The distribution of these events is concentrated within 2 km from the mainshock and delineates a sub-vertical «cloud» (fig. 5a). A few deeper events are spread below the mainshock. From the cross-sections in fig. 5a, we can infer that the rupture occurred along a subvertical plane, possibly with a SW-NE strike.

For the 25 events we obtain an average ERH=0.16 km with a maximum value of 0.4 and an average ERZ=0.46 km with a maximum of 1.2 km, belonging only to two events (see table III). The hypocentral locations of the Savoia di Lucania sequence evaluated in this study using the SAPTEX and RSNC network are substantially improved with respect to those by Cucci *et al*. (2004) that report the maximum location errors of 1.9 km both for the horizontal coordinates and for the depths, with four events with larger vertical errors.

A significant swarm of 19 earthquakes, named Moliterno in table III and fig. 5b, occurred along the S-SE side of the upper Agri Valley in an area of 3 km×5 km (fig. 4). It started on February 8, 2002 and lasted until December 2002 (end of the period investigated in this study). After four months of seismicity with ten events not larger than M_d 2.8, there was a period of quiescence (June-September). Then, the seismic activity increased again starting from October 2002 with events closer in time and maximum magnitude of 3.2. Most of the hypocenters are concentrated at the depth interval between 3 km and 7 km (fig. 5b). The distribution of earthquakes does not fully constrain the fault-plane geometry, although a slight elongation of the epicenters in a WNW-ESE direction is observed (fig. 5b). Moreover, it is noteworthy that this swarm is adjacent to the seismic sequence which occurred in 1996 just to the northwest. A detailed analysis of the 1996 sequence was carried out by Cucci *et al*. (2004), defining characteristics in terms of epicentral distribution, depths and magnitudes. These characteristics are very similar to those observed for the Moliterno swarm analyzed in this study.

Moving out from the region of the chain, we find changes in the pattern of crustal seismicity and define the second region at the eastern outer margin of the chain and in the foredeep (fig. 4). This region is characterized by broader and less frequent seismicity with deeper hypocenters ranging from 15 to 40 km (vertical cross sections AB and CD in fig. 4). Four isolated earthquakes locate within the foreland-foredeep, the Murge

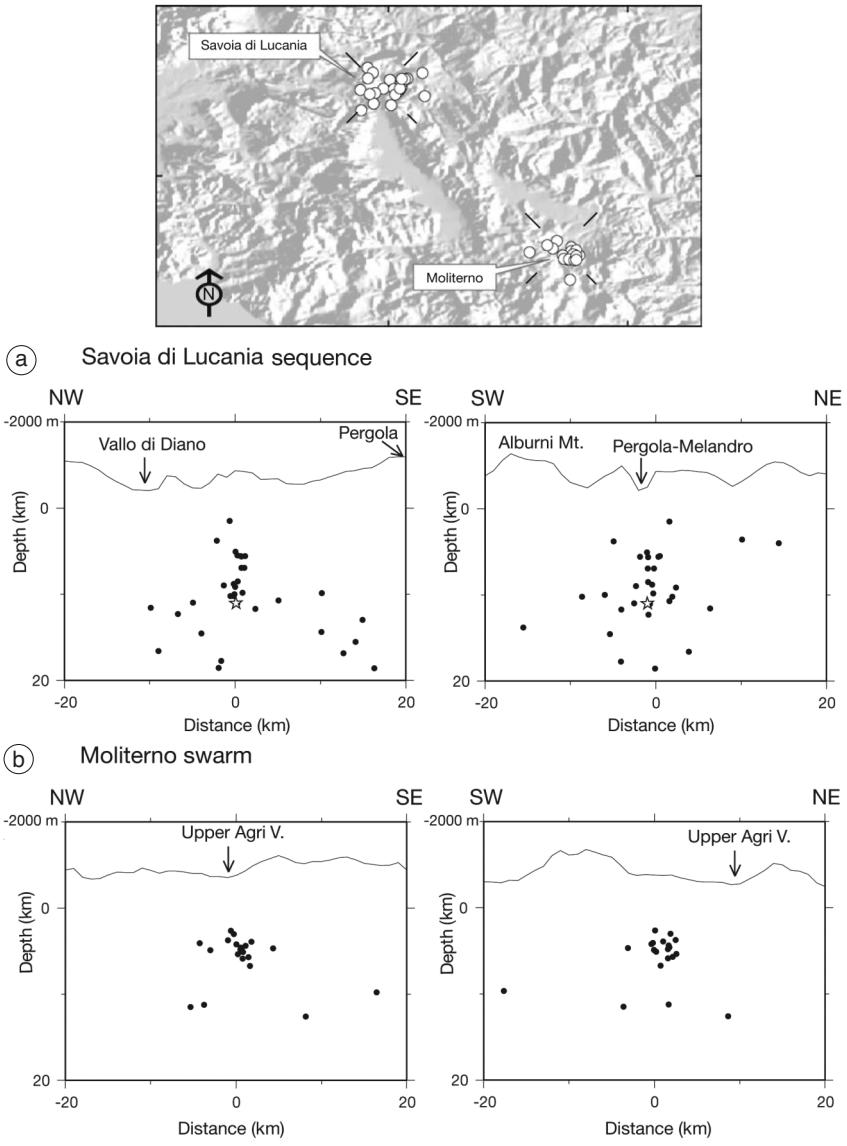

Fig. 5a,b. Epicentral locations and depth distribution of the a) Savoia di Lucania and b) Moliterno seismic sequences. Star indicates the mainshock hypocenter of the Savoia di Lucania sequence. Topography is vertically exaggerated.

and Andria-Trani area (fig. 4), with depths larger than 20 km, except for the shallower Andria event. The only sequence recorded is located beneath the Bradano foredeep area. This sequence, named Basentano in table III and fig. 4, consists of 5 events with depth ranging between 26 and 33 km, and maximum magnitude of 3.3 belonging to the westernmost event (fig. 4, vertical

cross section CD). These few events do not allow us to constrain the geometry of the seismogenic structure.

At the northwestern sector of the study area, we observe a partial overlap of the shallow and deep crustal seismicity beneath the edge of the chain at depths between 15 and 25 km (fig. 4, vertical cross section AB). This overlap does not occur to the south where the shallow and the deep hypocenters are adjacent but remain away from each other (fig. 4, vertical cross section CD).

Subcrustal earthquakes have also been recorded. Five out of six have hypocenters ranging from 37 to 45 km depth. They are not clustered; four are located to the east of the

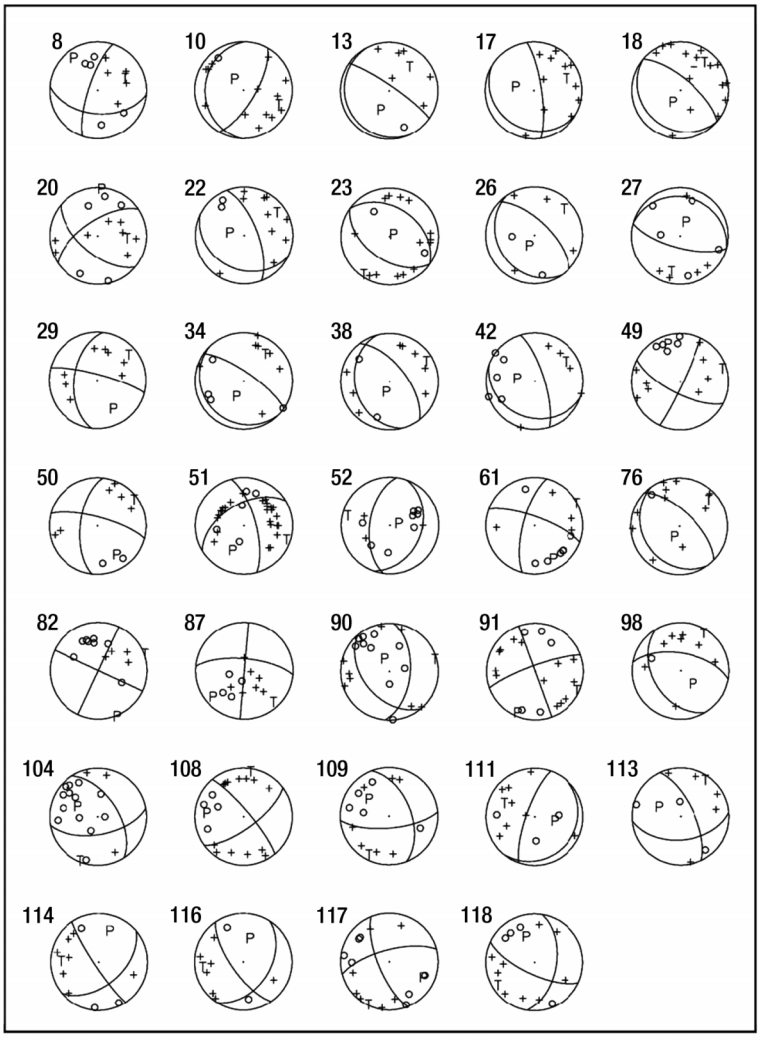

Fig. 6. Focal mechanisms computed with first motion polarities for 34 selected events. Event number corresponds to that in table III.

Table IV. Parameters of the computed fault-plane solutions. Event numbers correspond to those in table III. It is reported the strike, dip and rake of one of the two nodal planes, number of polarities, quality factor (Q_f, Q_p, see also table V) and stress regime categories (FPS): normal faulting (NF), predominately normal with strike-slip component (NS), strike-slip faulting (SS) and predominately thrust with strike-slip component (TS).

No.	Date	O.T.	Strike	Dip	Rake	No. Polarities	Q_f	Q_p	FPS
8	14/09/01	08:02	95	50	160	10	A	A	SS
10	30/09/01	23:44	30	70	−80	14	A	A	NF
13	13/10/01	18:57	155	10	−60	7	A	B	NF
17	04/11/01	10:22	120	20	−140	11	A	A	NF
18	04/11/01	10:28	130	20	−90	16	B	A	NF
20	13/11/01	13:21	130	60	150	13	A	B	TS
22	21/11/01	06:21	115	30	−130	12	A	A	NF
23	09/12/01	12:15	125	50	−90	16	B	A	NF
26	02/01/02	02:09	145	25	−80	6	A	A	NF
27	02/01/02	02:17	105	70	−90	10	B	A	NF
29	15/01/02	00:06	285	80	−140	8	A	A	SS
34	08/02/02	04:38	135	15	−80	11	B	A	NF
38	26/02/02	17:12	165	30	−70	10	A	B	NF
42	17/03/02	04:53	110	25	−140	10	B	A	NF
49	13/04/02	08:44	25	85	−20	13	A	B	SS
50	13/04/02	10:48	285	75	−150	8	A	B	SS
51	13/04/02	17:04	345	70	−140	25	B	A	NS
52	13/04/02	17:16	20	35	−80	11	B	A	NF
61	18/04/02	22:58	290	75	−160	12	A	B	SS
76	04/05/02	09:41	145	25	−80	11	B	B	NF
82	12/05/02	20:20	295	90	180	12	A	A	SS
87	07/06/02	05:47	275	70	0	11	B	A	SS
90	11/06/02	20:02	5	55	−60	18	B	A	NF
91	18/06/02	23:31	340	90	−170	19	A	A	SS
98	18/07/02	08:28	280	60	−120	9	A	A	NF
104	03/09/02	01:45	80	60	−140	16	B	A	NS
108	04/10/02	22:58	320	80	−20	18	A	A	SS
109	06/10/02	02:43	85	70	−140	12	B	A	NS
111	17/10/02	15:19	40	15	−70	11	B	B	NF
113	09/11/02	01:53	85	50	−150	8	A	A	NS
114	19/11/02	16:53	50	50	−10	10	A	A	SS
116	29/11/02	10:54	145	70	−130	9	A	A	NS
117	30/11/02	01:19	255	70	−160	14	A	A	SS
118	30/11/02	17:33	115	70	−140	13	B	A	NS

chain (the lower Agri Valley – 45 km, the lower Basentano Valley – 38 km, the Murge Tarantine – 42 km, southeast of Potentino area – 42 km) and one is in the Lao Valley – 41 km, close to the Tyrrhenian coast (fig. 4). A single 92 km-deep event was located within the Southern Tyrrhenian subduction zone near the Castelluccio area. This event reasonably belongs to the

sparse seismicity that characterizes the northern edge of the subduction zone (depth range 50-150 km, Frepoli *et al*., 1996).

2.2. *Focal mechanisms computation*

We computed best fit double-couple focal mechanisms using the fault-plane fit grid-search algorithm (FPFIT) of Reasenberg and Oppenheimer (1985). We selected 34 out of 120 focal mechanisms (fig. 6 and table IV) on the basis of quality factors Q_f and Q_p ranging from A to C for decreasing quality (table V). Q_f reflects the solution prediction misfit of the polarity data F_j, while Q_p reflects the solution uniqueness in terms of 90% confidence regions on strike, dip and rake. All solutions with one or both quality factors equal to C were rejected. Most of the fault-plane solutions show more than 10 polar-

Table V. Fault-plane solution quality factors Q_f and Q_p. F_j is the solution prediction misfit to the polarity data; Δstr, Δdip, Δrake are ranges of variability of strike, dip and rake, respectively.

	Q_f		Q_p
A	$F_j \leq 0.025$	A	Δstr, Δdip, Δrake ≤ 20°
B	$0.025 < F_j \leq 0.1$	B	20° to 40°
C	$F_j > 0.1$	C	>40°

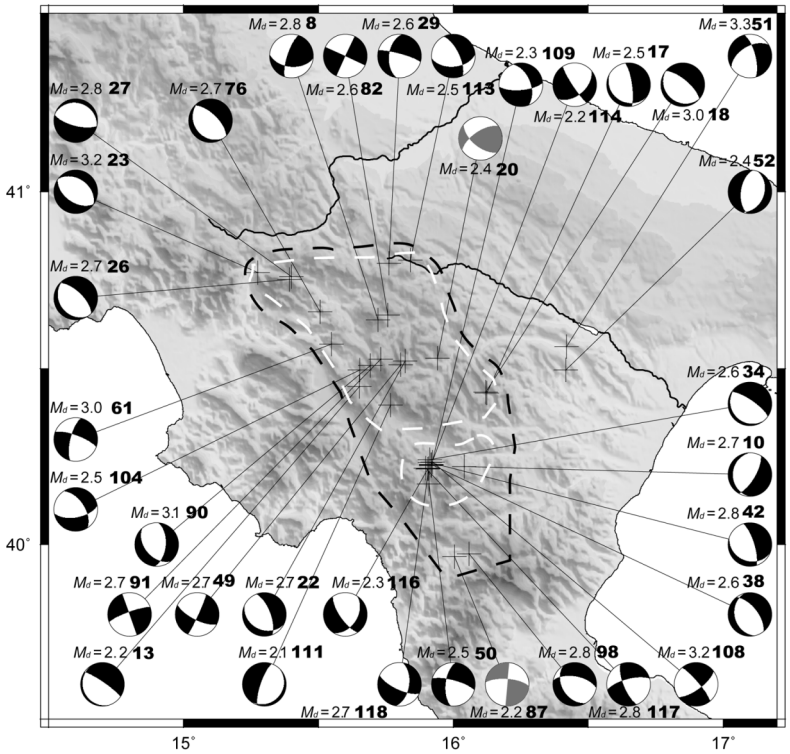

Fig. 7. Map showing the distribution of the 34 selected fault-plane solutions. Focal mechanisms in grey belongs to the subcrustal events. Duration magnitude and event number of table III and table IV are shown close to each fault-plane solution. Black dashed line encircle the crustal volume considered for the total stress inversion, while the two white dashed lines encircle the two sub-volumes considered for the further stress inversions (see text for explanation).

ities (table IV) and narrow azimuthal gap (<180°, see table III). We could compute and obtain constrained mechanisms even for events with magnitudes lower than 3.0, due to the dense seismic network.

Plunges of *P*- and *T*-axes were used to divide our data set into four main stress regime categories (Zoback, 1992). Following this classification (see table IV), 22 out of 34 focal mechanisms show prevalently normal fault solutions [16 are almost pure normal faulting (NF) and 6 are predominately normal with strike-slip component (NS)] while 11 are almost pure strike-slip solutions (SS) and only one event shows a prevalent thrust fault mechanism with strike-slip component (TS, event 20 in table III). This thrust solution event occurs below the crust at 42 km of depth, and is located at the eastern outer margin of the chain (fig. 7). Most of the computed focal solutions belong to the Apenninic Chain sector (fig. 7), and are associated with events shallower than 20 km. Their *T*-axes are prevalently NE-SW oriented. Only seven out of 32 fault-plane solutions of crustal events show *T*-axis orientation ranging from NW-SE to E-W (events number 10, 51, 52, 91, 111, 114, 116 in table III). The focal mechanism of the event at the intermediate depth of 92 km (number 87 in table III), which belongs to the northern portion of the Southern Tyrrhenian subduction zone, shows a *P*-axis plunge to the SW. We do not show the focal solutions relative to the events of the Savoia di Lucania sequence since they were not well constrained.

3. Fault-plane solution inversion for regional stress information

There is no correspondence between *P*- and *T*-axes of just a single fault-plane solution and the orientation of the maximum ($\sigma 1$) and minimum ($\sigma 3$) compressive stress directions (McKenzie, 1969). The brittle shallow crust generally contains small preexisting faults of any orientation that may have low frictional coefficients. There is slip on these faults when a small component of the shear stress is resolved along the fault surface. In order to have a mechanical consistency between the stress and the slip direction, the maximum ($\sigma 1$) and minimum ($\sigma 3$) compressive stress directions must be oriented somewhere within the dilatational and compressional quadrants, respectively, of the double-couple seismic radiation pattern.

All the developed inverse techniques used for finding the uniform stress field from a heterogeneous set of fault-plane solution data, resolve four of the six parameters of the stress tensor (Angelier, 1979, 1984; Gephart and Forsyth, 1984; Michael, 1984, 1985, 1987; Gephart, 1990a; Rivera and Cisternas, 1990). The unit vectors which define the orientation of the maximum ($\sigma 1$), intermediate ($\sigma 2$) and minimum ($\sigma 3$) compressive stress axis, and the factor shape $R = \sigma 2 - \sigma 1 / \sigma 3 - \sigma 1$ which describes the relative magnitudes of the principal stresses. Thus factor shape *R* constrains the shape of the stress ellipsoid. The inverse techniques of focal solution data cannot determine the absolute magnitude of the deviatoric and isotropic stresses, but they only identify the best stress tensor model that most closely matches all the fault-plane solutions of the source region. The basic assumption is that the deviatoric stress tensor is uniform over the studied crust volume and during the investigated time interval. The Focal Mechanism Stress Inversion program (FMSI) of Gephart (1990b) defines discrepancies between stress tensor orientation and observations by a misfit measure. The misfit of a single focal mechanism is defined as the minimum rotation about any arbitrary axis that brings one of the nodal planes and its slip direction into an orientation that is consistent with the slip direction predicted by a given stress model. The procedure uses a grid search technique operating in the whole space of stress parameters (stress directions and *R*). In this way the method finds the stress tensor that minimizes the average of misfits relative to all the fault-plane solutions.

We apply the Gephart (1990b) procedure to our data set of Southern Italy fault-plane solutions of crustal earthquakes, with the purpose of investigating the stress field in the region at a greater level of detail than in the previous studies (*e.g.*, Frepoli and Amato, 2000; Montone *et al.*, 2004). We assume a uniform stress field within the crust (2-25 km depth). The two focal mechanisms of the Basentano sequence (28 and

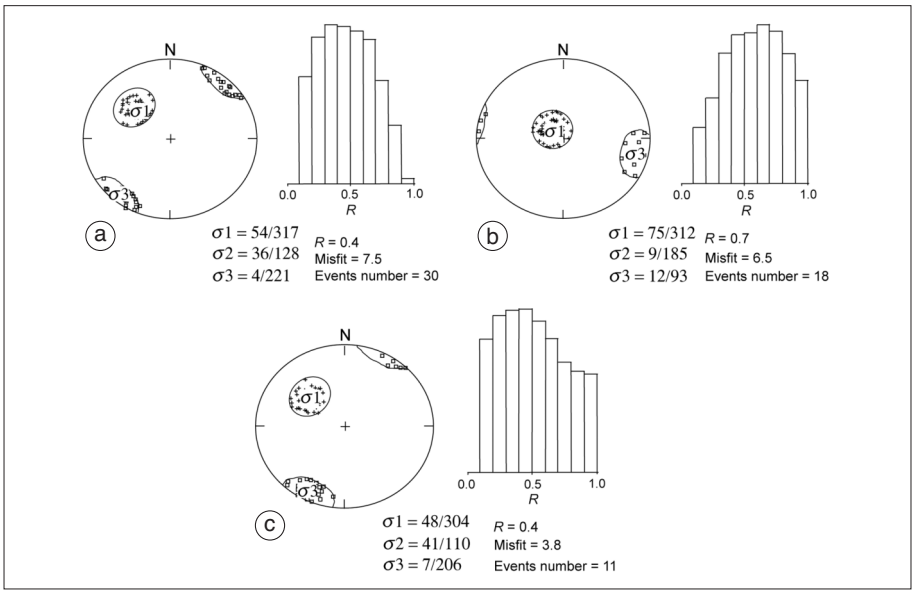

Fig. 8a-c. Stress inversion results using: a) 30 solutions; b) 18 solutions within the northern sector (Irpinia-Potentino-Savoia di Lucania-Calvello); c) 11 solutions of earthquakes within the southern sector (Moliterno-S. Martino d'Agri). For the location of the two sectors see fig. 7. For each inversion is shown the stereonet plot with the 95% confidence limits for $\sigma 1$ (small crosses) and $\sigma 3$ (small squares) and the histogram illustrating the uncertainty in the parameter R. Plunge and trend for the three principal stress axes are shown below the histograms.

32 km of depth, respectively) were not considered for stress inversion because they are far away from the area where the most of the seismicity is concentrated (fig. 7). Because of variations in the quality of fault-plane solution estimates, we use a focal mechanism weighting scheme based on the quality factors described in the previous section «Focal mechanisms computation». Weights of 4 were assigned to (Q_f, Q_p)= =(A, A) solutions, weights of 2 to (A, B) and (B, A) solutions, and weights of 1 to (B, B) solutions (table V). Larger weights provide more influence on the angular model misfit determinations. Moreover, an additional weight is given to the stronger events: 2 for events with magnitude equal to or larger than 3.1.

Stress inversion with the 30 fault-plane solutions dataset (fig. 8a; the events selected are within the dashed black line in fig. 7) shows a nearly horizontal NE-SW minimum compressive stress axis ($\sigma 3$) (plunge 4°, trend 221°), while maximum compressive axis ($\sigma 1$) is quite oblique (plunge 54°, trend 317°). The R value of 0.4 indicates that the $\sigma 2$ amplitude lies almost in the middle of the range defined by $\sigma 1$ and $\sigma 3$. Minimum average misfit is quite large (7.5).

According to Wyss *et al*. (1992), average misfit values larger than 6.0 may be due to an inhomogeneous stress distribution within the considered crustal volume. For this reason, we perform two new inversions dividing the 30 events total dataset into two sub-volumes (see the two dashed white lines in fig. 7): one to the north, including the Potentino-Irpinia-Savoia di Lucania area, with 18 focal mechanisms, and the other to the south, relative to the Moliterno swarm, with 11 events.

The results of the northern sector inversion (fig. 8b) show a stress orientation quite different from that of the whole dataset. The minimum compressive stress axis ($\sigma 3$) has plunge 12° and trend 93°, while the $\sigma 1$ is almost vertical with 75° of plunge and 312° of trend. The scalar R is 0.7 indicating that the intermediate

compressive stress axis ($\sigma 2$) tends to be closer to the minimum axis ($\sigma 3$). The quite large misfit value (6.5) indicate a small heterogeneity inside the northern sector.

The Moliterno sub-volume inversion (fig. 8c) shows a slightly northward rotation of the stress tensor (~15°) with respect to that resulting from the inversion of the whole dataset (fig. 8a). The minimum compressive stress axis ($\sigma 3$) shows a 7° of plunge and a 206° of trend, while the maximum one ($\sigma 1$) has plunge 48° and trend 304°. The homogeneous tectonic regime (very small misfit) results from the inversion of focal mechanisms of the closely spaced events of the Moliterno swarm.

4. Discussion and conclusions

In this paper we presented a detailed study of the seismicity in the Lucanian Region during the period June 2001-December 2002. We gathered the digital waveforms from two seismic networks: the RSNC and the temporary SAPTEX networks. To these data we added the *P*- and *S*-arrival times of the events recorded by the Eni-Agip local network in the upper Agri Valley, to further improve earthquake location in that area. The resulting hypocentral locations are well constrained and reasonably improved with respect to those obtained by only RSNC data. This is due to the large number of stations and to the closely spaced array used to locate the low magnitude seismicity of the Lucanian Region.

During the observed period most of the seismicity was concentrated within the Apenninic Chain (fig. 4). Conversely, at the eastern margin of the chain and in the Bradano foredeep the seismicity was very sparse. Seismicity defines two main clusters: the first is confined in the Irpinia area and in the Pergola-Melandro Basin, the second to the south in the upper Agri Valley and the Castelluccio area. Between these two areas, there is a region with a lack of shallow events and with only a few earthquakes occurring at depths of more than 10 km (see section EF in fig. 4). The western portion of the study region (Cilento and Policastro Gulf) is characterized by an absence of crustal earthquakes. The spatial distribution of the earthquakes we examined closely follows the pattern delineated by the seismicity of the last two decades (fig. 1). Then, despite the short time interval, the seismicity analyzed in this paper would be representative of the seismic behavior of the Lucanian Region for such magnitudes even in longer order of time.

The relocated seismicity allows us to better discriminate the crustal regions characterized by shallow seismicity (within the first 20 km of depth) from those with deeper events (>20 km depth) (see cross-sections in fig. 4). As a general remark, seismicity deepens moving towards the external margin of the chain. Indeed, crossing the Lucanian Region from SW to NE, we observe hypocentral depths that increase from about 20 km, along the chain, to about 30 km in the Bradano foredeep. Our results relative to the events in and around the area of the 1990 Potenza sequence (Potentino area) and to the events in the Basentano area, whose hypocentral depths were in the range of 15 to 27 km and 26 to 33 km respectively (see table III), definitively stress that the outer margin of the Lucanian Apenninic Chain and the Bradano foredeep area are characterized by deep crust seismicity. Within the external area and the foredeep, we also recorded four isolated subcrustal events (fig. 4).

Figure 9 shows the earthquake hypocenters located in the northwestern portion of the study area (section AB in fig. 4) superimposed on the geological-structural interpretation by Merlini and Cippitelli (2001) of a seismic line crossing the northern sector of the Vallo di Diano. The resulting section suggests that most of the upper crust earthquakes clusters in the brittle carbonate of the Apulian platform, and sparse events occur deeper in the basement as previously described; no background seismicity is apparently located in the shallower layers of the unit of the Lagonegro Basin.

Fault-plane solutions are used to retrieve the stress tensor orientation. The stress inversion relative to the crustal earthquakes (fig. 8a) reveals that the Lucanian Apennine is generally ongoing through NE-SW extension, like the rest of the Apenninic Chain (Pondrelli *et al.*, 1998; Frepoli and Amato, 2000; Cucci *et al.*, 2004; Montone *et al.*, 2004, among many others). However, local heterogeneity in the stress

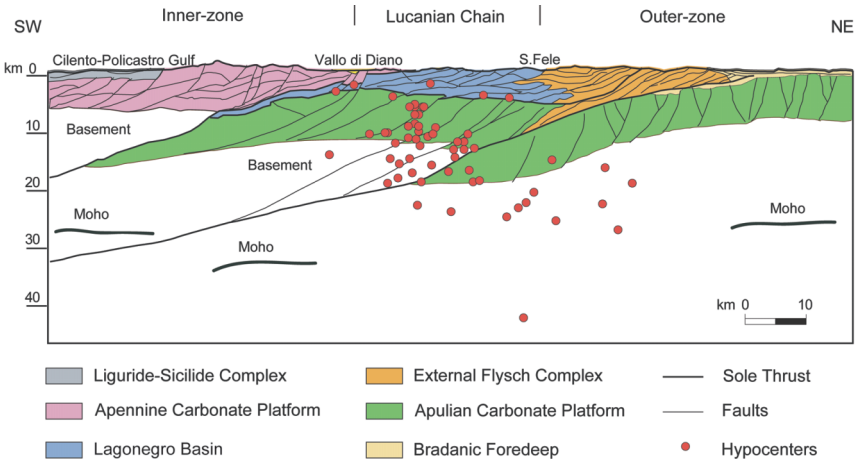

Fig. 9. Crustal and subcrustal seismicity (section AB in fig. 4) superimposed on the geological and structural interpretation of a NE-SW oriented seismic line (modified by Merlini and Cippitelli, 2001).

orientation results from the fairly large average misfit, that was not previously identified.

In order to analyze this stress heterogeneity within the selected area (black dashed line in fig. 7), we divided the dataset and separately inverted the solutions belonging to the northern and the southern sectors of seismicity (white dashed lines in fig. 7). Concerning the northern sector, we obtain an almost E-W minimum compression stress axis ($\sigma 3$) and a small decreasing of the average misfit (fig. 8b). Despite the small amount of data and the relative large misfit, from this inversion a local rotation of the extensional axis in the area of the Vallo di Diano and Pergola-Melandro (figs. 4 and 7) can be inferred, from a regional NE-SW to an E-W direction.

The stress orientation of the southern sector of seismicity represents the local stress of the Moliterno swarm. For these swarms a small anticlockwise rotation of the minimum compressive axes ($\sigma 3$) is observed, being NNE-SSW oriented (fig. 8c) with respect to the total inversion (fig. 8a). Thus, it can be extrapolated that NNE-SSW extension occurred inside the crustal volume of the Moliterno swarm.

Through the analysis of event locations we obtain some details on the source geometry of a sequence and a swarm occurred in the study period within the Lucanian Chain. The spatial distribution of the Savoia di Lucania sequence well delineates a sub-vertical fault plane beneath the northern side of the Pergola-Melandro Basin between 4 and 11 km of depth (fig. 5a). The observations on earthquake distribution and fault geometry are consistent with the hypothesis of a secondary fault bounding the northern tip of the NNW-SSE to NW-SE trending major seismogenic structure within the Pergola-Melandro Basin (Valensise and Pantosti, 2001; Moro *et al*., 2003; Lucente *et al*., 2005). The background seismicity such as that of the Savoia di Lucania sequence mostly develops at the border of the main NW-oriented fault segment (Bisio *et al*., 2004; Chiarabba *et al*., 2005).

The cross-sections of the Moliterno swarm show a hardly perceptible high-dipping structure, between 3 and 7 km in depth. This swarm is located just to the ESE of that recorded in 1996 and analyzed by Cucci *et al*. (2004). The NE-SW sections of this two upper Agri Valley sequences are quite similar in the fault plane geometry and suggests the presence, along the southwestern side of the Valley, of a NW-SE to WNW-ESE oriented, ~NE dipping source activated in two different periods. The stress inversion relative to the Moliterno swarm indicates

a NNE-SSW extensional regime (fig. 8c) that would be in agreement with the orientation of the inferred fault.

Our results stress that in the Lucanian Region there is eastward deepening of the hypocentral depths from inner to outer margin of the belt and foredeep (see cross sections in fig. 4) such as outlined by Chiarabba *et al*. (2005) for the external area of the Northern and Central Apennines system. The trend of the hypocentral depths delineated by the present study indicates a deeper boundary between the brittle and ductile crust beneath the external margin of the Lucanian Apennine and the foredeep, with respect to that beneath the chain itself. This different crustal setting is also suggested by tomographic and geothermal gradient studies that indicate for the outer and inland regions a brittle/ductile limit at 28-30 km and at 15-18 km, respectively (Chiarabba and Amato, 1996; Harabaglia *et al*., 1997). Chiarabba *et al*. (2005) report that the increasing seismogenic layer depth follows the flexure of the Adria and Ionian lithosphere; despite the short period of detection, the pattern of deep crustal and subcrustal seismicity recorded in the eastern portion of the Lucanian Region might be similarly interpreted.

Acknowledgements

We thank Eni-Agip for providing the *P*- and *S*-wave arrival times of the Agri Valley seismic network. We are grateful to Francesca Di Luccio for the suggestions and the fruitful comments on the work.

REFERENCES

AMATO, A. and G. SELVAGGI (1993):, Aftershock location and *P*-velocity structure in the epicentral region of the 1980 Irpinia earthquake, *Ann. Geofis.,* **XXXVI** (1), 3-25.

ANGELIER, J. (1979): Determination of the mean principal directions of stresses for a given fault population, *Tectonophysiscs*, **56**, T17-T26.

ANGELIER, J. (1984): Tectonic analysis of fault slip data sets, *J. Geophys. Res*., **89**, 5835-5848.

AZZARA, R., A. BASILI, L. BERANZOLI, C. CHIARABBA, R. DI GIOVAMBATTISTA and G. SELVAGGI (1993): The seismic sequence of Potenza (May 1990), *Ann. Geofis*., **XXXVI** (1), 237-243.

BISIO, L., R. DI GIOVAMBATTISTA, G. MILANO and C. CHIARABBA (2004): Three-dimensional earthquake locations and upper crustal structure of the Sannio-Matese region (Southern Italy), *Tectonophysics*, **385**, 121-136.

BOSCHI, E., D. PANTOSTI, D. SLEJKO, M. STUCCHI and G. VALENSISE (Editors) (1990): Irpinia dieci anni dopo, *Ann. Geofis*., **XXXVI** (1), pp. 363.

CASTELLO, B., G. SELVAGGI, C. CHIARABBA and A. AMATO (2005): *CSI Catalogo della Sismicità Italiana 1981-2002*, versione 1.0. (INGV-CNT, Roma), (on line: http://www.ingv.it/CSI/).

CHIARABBA, C. and A. AMATO (1996): Crustal velocity structure of the Apennines (Italy) from *P*-wave travel time tomography, *Ann. Geofis*., **XXXIX** (6), 1133-1148.

CHIARABBA, C., L. JOVANE and R. DI STEFANO (2005): A new view of Italian seismicity using 20 years of instrumental recordings, *Tectonophysics*, **395**, 251-268.

CIMINI, G.B., P. DE GORI and A. FREPOLI (2005): Passive seismology in Southern Italy: the SAPTEX array, *Ann. Geophysics*, **49** (2) (in press).

CPTI WORKING GROUP (1999): *Catalogo Parametrico dei Forti Terremoti Italiani* (GNDT-ING-SGA-SSN), (Ed. Compositori, Bologna), pp. 88.

CUCCI, L., S. PONDRELLI, A. FREPOLI, M.T. MARIUCCI and M. MORO (2004): Local pattern of stress field and seismogenic sources in the Pergola-Melandro Basin and the Agri Valley (Southern Italy), *Geophys. J. Int*., **156** (3), 575-583.

DI BUCCI, D. and S. MAZZOLI (2003): The October-November 2002 Molise seismic sequence (Southern Italy); an expression of Adria intraplate deformation, *J. Geol. Soc. London*, **160** (4), 503-506.

DI LUCCIO, F., E. FUKUYAMA and N.A. PINO (2005): The 2002 Molise earthquake sequence: what can we learn about the tectonics of Southern Italy?, *Tectonophysics* **405**, 141-154.

EKSTRÖM, G. (1994): Teleseismic analysis of the 1990 and 1991 earthquakes near Potenza, *Ann. Geofis*., **XXXVII** (6), 1591-1599.

FREPOLI, A. and A. AMATO (2000): Spatial variation in stresses in Peninsular Italy and Sicily from background seismicity, *Tectonophysiscs*, **317**, 109-124.

FREPOLI, A., G. SELVAGGI, C. CHIARABBA and A. AMATO (1996): State of stress in the Southern Tyrrhenian subduction zone from fault-plane solutions, *Geophys. J. Int*., **125**, 879-891.

GEPHART, J. (1990a): Stress and the direction of slip on fault planes, *Tectonics*, **9**, 845-858.

GEPHART, J. (1990b): FMSI: a FORTRAN program for inverting fault/slickenside and earthquake focal mechanism data to obtain the regional stress tensor, *Comput. Geosci*., **16**, 953-989.

GEPHART, J. and W. FORSYTH (1984): An improved method for determining the regional stress tensor using earthquake focal mechanism data: application to the San Fernando earthquake sequence, *J. Geophys. Res*., **89**, 9305-9320.

HARABAGLIA, P., F. MONGELLI and G. ZITO (1997): Geothermics of the Apenninic subduction, *Ann. Geofis*., **XL** (5), 1261-1274.

LAHR, J.C. (1989): HYPOELLIPSE/Version 2.0: a computer program for determining local earthquake hypocentral

parameters, magnitude, and first motion pattern, *U.S. Geol. Surv. Open File Rep*. *95*, 89-116.

LUCENTE, F.P., N. PIANA AGOSTINETTI, M. MORO, G. SELVAGGI and M. DI BONA (2005): Possible fault plane in a seismic gap area of the Southern Apennines (Italy) revealed by receiver function analysis, *J. Geophys. Res*., **110** (B04307), doi: 10.1029/2004JB003187.

MCKENZIE, D.P. (1969): The relation between fault-plane solutions for earthquakes and the directions of the principal stresses, *Bull. Seismol. Soc. Am*., **59** (2), 591-601.

MERLINI, S. and G. CIPPITELLI (2001): Structural styles inferred by seismic profiles, in *Anatomy of an Orogen: the Apennines and Adjacent Mediterranean Basins*, edited by G.B. VAI and I.P. MARTINI (Kluwer Academic Publishers), 441-454.

MICHAEL, A. (1984): Determination of stress from slip data: faults and folds, *J. Geophys. Res*., **89**, 11517-11526.

MICHAEL, A. (1985): Regional stress and large earthquakes: An observational study using focal mechanisms, *Ph.D. Thesis* (Stanford University, Stanford, California).

MICHAEL, A. (1987): Use of focal mechanisms to determine stress: a control study, *J. Geophys. Res*., **92**, 357-368.

MICHETTI, A.M., L. FERRELLI, E. ESPOSITO, E. PORFIDO, A.M. BLUMETTI, E. VITTORI, L. SERVA and G.P. ROBERTS (2000): Ground effects during the 9 september 1998, $M_w = 5.6$, Lauria earthquake and the seismic potential of the «aseismic» Pollino region in Southern Italy, *Seismol. Res. Lett*., **41** (1), 31-46.

MONTONE, P., M.T. MARIUCCI, S. PONDRELLI and A. AMATO (2004): An improved stress map for Italy and surrounding regions (Central Mediterranean), *J. Geophys. Res*., **109** (B10410), doi: 10.1029/2003JB002703.

MORO, M., L. AMICUCCI, F.R. CINTI, F. DOUMAZ, P. MONTONE, S. PIERDOMINICI and M. SAROLI (2003): Evidence for Late Pleistocene-Holocene Activity along a Potential Seismic Source in Southern Apennines (Italy), *Eos Trans. Am. Geophys. Un*., **84** (46), T51D-0199.

PONDRELLI, S., A. MORELLI and G. EKSTRÖM (1998): Moment tensors and seismotectonics of the Mediterranean region, *Ann. Geophysicae*, **16** (suppl. I), C19.

PONDRELLI, S., A. MORELLI, G. EKSTRÖM, S. MAZZA, E. BOSCHI and A.M. DZIEWONSKI (2002): European-Mediterranean regional centroid-moment tensors: 1997-2000, *Phys. Earth Planet. Int*., **130**, 71-101 (Quick Regional CMT available at: http://mednet.ingv.it/events/QRCMT/Welcome.html).

REASENBERG, P. and D. OPPENHEIMER (1985): FPFIT, FPPLOT and FPPAGE: FORTRAN computer programs for calculating and displaying earthquake fault-plane solutions, *U.S. Geol. Surv. Open-File Rep*. 85-739.

RIVERA, L. and A. CISTERNAS (1990): Stress tensor and fault-plane solutions for a population of earthquakes, *Bull. Seismol. Soc. Am*., **80**, 600-614.

VALENSISE, G. and D. PANTOSTI (Editors) (2001): Database of potential sources for earthquakes larger than *M* 5.5 in Italy, *Ann. Geofis*., **44** (suppl. to no. 4), pp. 180 (with CD-ROM).

VALENSISE, G., D. PANTOSTI and R. BASILI (2004): Seismology and tectonic setting of the 2002 Molise, Italy, earthquake, *Earthquake Spectra*, **20**, S23.

WYSS, M., LIANG, B., W.R. TANIGAWA and X. WU (1992): Comparison of orientations of stress and strain tensors based on fault-plane solutions in Kaoiki, Hawaii, *J. Geophys. Res*., **97**, 4769-4790.

ZOBACK, M.L. (1992): First- and second-order patterns of stress in the lithosphere: the World Stress Map Project, *J. Geophys. Res*., **97** (B8), 11703-11728.

(received September 12, 2005;
accepted November 4, 2005)